Gouma and Wang, J Material Sci Eng 2015, 4:3
DOI: 10.4172/2169-0022.1000165

Journal of Material Sciences & Engineering

Research Article Open Access

Flame Spray Synthesis of WO_3 for No Breath Monitors

Gouma PI* and Wang L

Center for Nanomaterials and Sensor Development, SUNY Stony Brook, NY11794, USA

Abstract

The γ-phase polymorph of WO_3 has been established in the literature as a selective NO sensor. When processed at the nanoscale, this material shows high sensitivity to trace levels of NO gas. Thus, it is intended for use in breath monitors of NO in exhaled breath to diagnose asthma. Focusing on the economic and scalable synthesis of this material, this paper reports on the flame-spray processing of WO_3 nanopowders of the monoclinic γ-phase. Structural and chemical characterization of as-sprayed and heat-treated nanopowders were carried out that revealed the conditions for tailored phase and particle size distribution suitable for the intended application of this material in breath-based diagnostics.

Keywords: Flame spray pyrolysis; WO_3 polymorphs; Nanostructured oxide; Nitric oxide detector

Introduction

Nitric oxide belongs to the class of inorganic gaseous chemicals found in exhaled breath and is characterized as a signaling biomarker for disease [1-3]. The diagnostic value of exhaled NO measurements to differentiate between healthy persons with or without respiratory symptoms and patients with confirmed asthma has been established by Dupont who showed that >16 ppb of NO in lower respiratory tract could be treated as a cutoff for asthma with a 90% specificity and 90% positive predictive value [4]. This suggests that a simple and non-invasive measurement of exhaled NO may provide a reliable signal for asthma diagnosis.

Breathalyzer prototypes utilizing NO selective nanostructured sensors to detect and monitor the fractional nitric oxide concentration (FENO) in breath have been demonstrated and patented by our group [5,6]. The next challenge has been to produce the NO sensing elements (i.e. nanocrystals of γ-WO_3) using a scalable process that will enable the use of the NO breathalyzer and asthma monitor as a home diagnostic tool. This manuscript describes the scaled up process used to synthesize γ-WO_3, by means of flame spray pyrolysis.

Flame-spray pyrolysis is a very effective method to synthesize nano-sized oxide particles in a large amount and an excellent quality. It has been used for dry, one-step synthesis of catalysts, sensors, biomaterials, phosphors and even nutrional supplements [7]. Furthermore, FSP is a scalable process with proven production rates over 1 kg/h [8]. FSP-made nanoparticles can also be directly deposited onto sensor substrates. This paper provides a new recipe and specific process steps for obtaining the required oxide polymorph and to optimize the particle size distribution for NO sensing.

Experimental Methods

In this work, precursor solutions were prepared from ammonium tungstate hydrate ($H_{26}N_6O_{41}W_{12}$, Aldrich, purity >97%) diluted (0.4 mol/l of tungsten ions) in a 3:2 (volume ratio) mixture of diethylene glycol monbutyl ether ($C_8H_{18}O_3$ Fluka, >98.5%) and ethanol (C_2H_6O, Fluka, >99.5%). The solution was fed at 5 ml/min through the inner reactor capillary. Through the surrounding annulus, 5 l/min of oxygen (Pan Gas, purity >99%) were fed dispersing the precursor solution into a combustible spray. The methane and oxygen flow rates in the FSP-supporting premixed flame are 1.5 and 3.2 l/min, respectively.

X-ray diffraction (XRD) patterns were obtained with a Bruker AXS D8 Advance diffractometer (40 kV, 40 mA, Karlsruhe, Germany) operating with Cu K_α radiation. Phase analysis is accomplished using two softwares, namely DIFFRAC^{plus} EVA and DIFFRAC^{plus} TOPAS. Raman scattering spectra were recorded by Renishaw InVia Reflex Raman Spectrophotometer with the excitation laser length of 514.5 nm, laser power of 300 mW and exposure time of 30s at RT. SEM images are obtained with SEM, LEO 1550 SFEG Microscope operated at a voltage of 15 kV. TEM images were obtained on a CM30ST microscope, FEI (Eindhoven), LaB6 cathode, operated at 300 kV, SuperTwin lens, point resolution ~2 Å.

Results and Discussion

As-sprayed powders

The as-synthesized powder products resulted from the reaction shown below:

$$H_{26}N_6O_{41}W_{12} \xrightarrow{\text{flame}} W^{6+} \xrightarrow{O_2} WO_3$$

They were blue green in color. When a default setup without any accessories was applied, medium grain-sized WO_3 was obtained. (Sample A) The average surface area of such products is 63.0 m^2/g, (BET-determined particle diameter is 13 nm). Most peaks in the XRD spectrum shown in Figure 1a, (labeled as "middle grain size") can be indexed in stable-phase WO_3 polymorphs. However, due to the small size of the particles, most adjacent peaks overlap a lot. Thus, Raman spectroscopy was used to identify the phase composition of the product, as shown in Figure 1b. In this spectrum, peaks at 272, 324, 715 and 805 cm^{-1} correspond to monoclinic γ phase, the stable form of WO_3 at RT [9-11]. The band at 942 cm^{-1} can be assigned to the stretching mode of W=O terminal bonds indicating surface tungsten hydrates [10,11]. Peaks at 203, 272, 303, 370, 425, 642, 688 and 805 cm^{-1} belong to the ε phase of WO_3.

***Corresponding author:** Gouma PI, Center for Nanomaterials and Sensor Development, SUNY Stony Brook, NY11794, USA, Tel: 631-6324537; E-mail: pelagia-irene.gouma@stonybrook.edu

Received March 04, 2015; **Accepted** April 20, 2015; **Published** April 28, 2015

Citation: Gouma PI, Wang L (2015) Flame Spray Synthesis of WO_3 for No Breath Monitors. J Material Sci Eng 4: 165. doi:10.4172/2169-0022.1000165

Tungsten hydrates are common by-products during the synthesis of WO_3. However, the appearance of ε-WO_3 is surprising here since it was typically reported as a phase only stable below -40°C. Although not quantitative, the relative intensity of 642 cm^{-1} and 688 cm^{-1} bands compared to 715 cm^{-1} band indicates the content of ε-WO_3 in the products. It is clear that the as-synthesized product contains a fairly high percentage of ε-WO_3. Computer-assisted phase analysis based on the XRD spectrum enables us to quantitatively determine the fraction of either phase.

By using a cooling oxygen gas sheath around the flame, smaller grain-size particles were able to grow. As the quenching sheath diameter shrinks from 10 cm (Sample B2) to 5 cm (Sample B1), the particle diameter decreases from 12 nm (S=66.3 m^2/g) to 9 nm (S=97.0 m^2/g). Figure 1 shows the XRD and Raman spectra of the powders obtained having different grain sizes. For example, for Sample B1 (labeled as "small grain size") the shapes of the spectra obtained are similar to those of medium-sized particles, except that all the peaks in the XRD result are a little bit broader resulting from the smaller grain size of this batch. Besides, ε-WO_3 becomes a dominant phase in the material, as concluded from the enhanced intensity of ε-WO_3 peaks in the Raman result. In addition, the W=O bond peak is also intensified, showing a more active surface in this material, which can be attributed to the "nano effect".

On the other hand, the use of a glass tube on top of the flame enables the growth of particles. The diameters are 16 nm (S=52.5 m^2/g), 20 nm (S=40.5 m^2/g) and 27 nm (S=30.5 m^2/g) when the tube lengths are 10 cm (Sample C1), 20 cm (Sample C2) and 30 cm (Sample C3), respectively. Figure 1 also provides the structural information of Sample C3 (labeled as "large grain size"). Quite different from those of the other two products, the peaks in both XRD and Raman spectra become very sharp and easy to identify due to the large grain size of the material. The peaks that are unique to ε-WO_3 (JCPDS No.: 872386) become distinguishable from γ-WO_3 (JCPDS No.: 830950) for the first time. Its Raman spectrum reveals a much smaller fraction of ε-WO_3 in this product. Besides, the surface hydrate almost disappears in this product. As the grain size increases, a larger fraction of ε phase of WO_3 will appear in the as-synthesized products.

Figure 2 shows TEM images illustrating the morphology and crystal structures of the as-synthesized WO_3 products. Most particles share a spherical shape in (a) and (b). Their SAED patterns (d) and (e) are composed of a series of continuous diffraction rings per their nanocrystalline character. Those rings can be indexed in stable phases of WO_3. Since γ-WO_3 and ε-WO_3 are structurally similar, it is impossible to distinguish the rings from either phase. Compared to (e), the rings in (d) are more ambiguous due to the smaller size of the product. In Image (c), we can clear observe two major shapes in

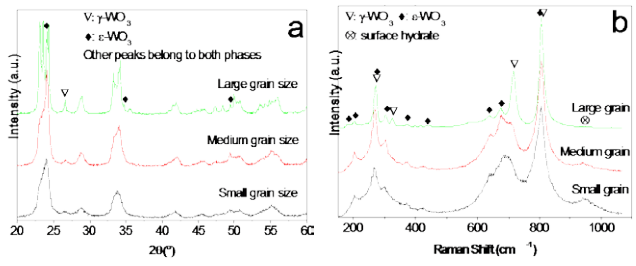

Figure 1: (a) XRD patterns and (b) Raman spectra, of the different batches of pure WO_3.

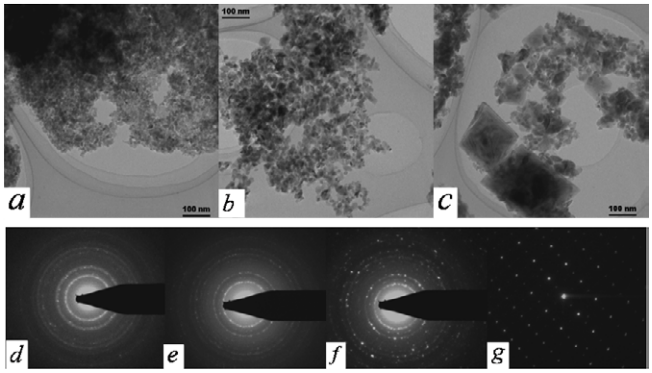

Figure 2: (a-c) TEM images of as-synthesized WO_3 nanoparticles and (d-g) their corresponding SAED patterns: (a) and (d) small grain size; (b) and (e) middle grain size; (c) and (f,g) large grain size.

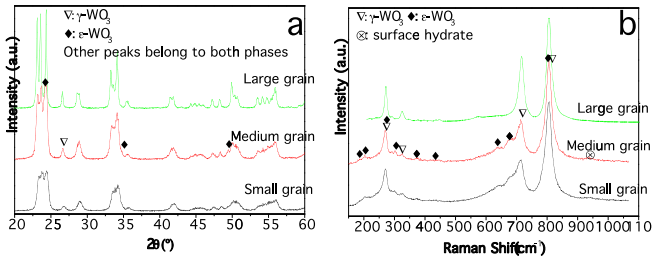

Figure 3: (a) XRD and (b) Raman spectra of heat-treated pure WO_3.

"large-grain-size" product. One is small round-shaped particles with an average diameter of 50 nm and the other is huge square mono-crystals whose sizes varying from 60 nm to 300 nm. SAED patterns reveal the small particles are polycrystalline WO_3 (Image (f)) and the huge crystals are single crystalline γ-WO_3 with crystal planes either (100) or (110) (Image (g)).

Heat-treated powders

All the synthesized products were heat treated at 500°C for 8 hours to let them stabilize. Heat treatment had a profound effect on the products. First of all, the color of the products changed to yellowish green as is typical of pure γ-WO_3 powders. Second, the particles sizes increased and grew almost twice the size of the as-sprayed products. Such variation is also reflected in the XRD and Raman spectra in Figure 3 in which most peaks became much sharper.

Finally and most importantly, following heat treatment, all pure WO_3 undergoes a phase transition, in which the ε-WO_3 phase transforms to γ phase. This is clearly shown in Figure 3. In the Raman spectra, the intensities of ε-WO_3 peaks were reduced. In large-grain-size products, they even disappeared. Figure 3 also provides evidence that the surface hydrates have also diminished after heat treatment. The color change results from the disappearance of both ε-WO_3 and surface hydrates.

Table 1 summarizes the structural and morphological features of the flame-sprayed powders obtained under variable processing conditions and before/after heat-treatment. The highest content of γ-phase is obtained for a larger particle size of about 60 nm. Since this polymorph is the NO-selective phase, C3 is expected to be the optimum material for developing gas sensing films for NO detection.

Sample No.	SA (m^2/g)		d_{BET} (nm)		γ-WO_3 ratio	
	before	after	before	after	before	after
B1	97.0	40.2	9	21	27.6	68.4
B2	66.3	33.8	12	25		
A	63.0	33.5	13	25	30.7	67.8
C1	52.5	29.8	16	28		
C2	40.6	20.2	20	41		
C3	30.5	13.6	27	61	68.7	97.8

Table 1: Particle size comparison of pure WO_3 before and after heat treatment.

Conclusion

Scalable synthesis of nanostructured powders of tungsten trioxide was accomplished by flame spray pyrolysis. Process maps that determine the relative phase content and particle sizes were obtained. Pure γ-WO_3 powders may be obtained in this manner. These are targeted as sensing elements for the detection of NO in exhaled breath for personalized asthma monitors.

Acknowledgment

This work has been funded by the National Science Foundation under the award: DMR-0304169.

References

1. Phillips M (1992) Breath tests in medicine. Sci Am 267: 74-79.
2. Yates DH (2001) Role of exhaled nitric oxide in asthma. Immunol Cell Biol 79: 178-190.
3. Cao WQ, Duan YX (2006) Breath analysis: Potential for clinical diagnosis and exposure assessment. Clin Chem 52: 800-811.
4. Dupont LJ, Demedts MG, Verleden GM (2003) Prospective evaluation of the validity of exhaled nitric oxide for the diagnosis of asthma. Chest 123: 751-756
5. Gouma PI, Kalyanasundaram K (2008) A Selective Nanosensing Probe for Nitric Oxide. Appl Phys Lett 93: 244102.
6. Gouma P (2012) Nanoceramic Sensors for Medical Applications. Am Ceram Soc Bulletin 91: 26-31.
7. Strobel R, Pratsinis SE (2007) Flame aerosol synthesis of smart nanostructured materials. J Mater Chem 17: 4743-4756.
8. Jossen R, Mueller R, Pratsinis SE, Watson M, Kamal Akhtar M (2005) Morphology and composition of spray-flame-made yttria-stabilized zirconia nanoparticles. Nanotechnology 16: S609-S617.
9. Ashraf S, Blackman CS, Palgrave RG, Naisbitta SC, Parkin IP (2007) Aerosol assisted chemical vapour deposition of WO_3 thin films from tungsten hexacarbonyl and their gas sensing properties. J Mater Chem 17: 3708-3713.
10. Daniel MF (1987) Infrared and Raman study of WO_3 tungsten trioxides and $WO_3.xH_2O$ tungsten trioxide hydrates. J Solid State Chem 67: 235-247.
11. Arai M, Hayashi S, Yamamoto K (1990) Raman studies of phase transitions in gas-evaporated WO_3 microcrystals. Solid State Commun 75: 613-616.